Tufa Deposits in the Mygdonian Basin (Northern Greece) studied with RMT/CSTAMT, VLF & Self-Potential

M. Gurk[1,2], A.S. Savvaidis[1], M. Bastani[3]
[1] Institute of Engineering Seismology and Earthquake Engineering (ITSAK), Greece
[2]Institut für Geophysik, Universität zu Köln, Germany
[3]Geological Survey of Sweden (SGU), Uppsala, Sweden

SUMMARY

During 2007, near surface EM geophysical soundings have been conducted to study tufa outcrops in the Mygdonian Basin. The presence of carbon rich hot springs in the eastern lake (Volvi) and various tufa outcrops in the northern rim of the basin supports our idea that the tufa genesis is connected down to lineamentic faults in the basement. More precisely, those deposits are preferentially located along fracture traces, either immediately above extensional fissures or in the hanging wall of normal faults. Hence, the distribution of the tufa at surface may delineate the fault distribution at depth and/or shows areas with increased basement fracturation. Analysing the present day geothermal regime allows to sketch a hydrogeological model based on neotectonic seismic activities in the past.

Keywords: Travertine, Tufa, Self-Potential, streaming electrical potential, RMT, CSTAMT, VLF, Mygdonian basin, geothermal area, normal faulting

INTRODUCTION

The Mygdonian basin, situated between the two lakes Volvi and Lagada ca. 45 km east of Thessaloniki (Fig. 1), is a neotectonic graben structure (5 km wide) with increased seismic activity along distinct normal fault patterns (Papazachos et al., 1979; Karagianni et al., 1999; Goldsworthy et al., 2002). Fluvioterrestrial and lacustrian sediments (approx. 350-400 m thick) are overlying the basement consisting of gneiss with several marble bands embedded between amphiboles, limestones, quartzites or phyllites.
The presence of carbon rich hot springs in the eastern lake (Volvi) and various tufa outcrops in the northern rim (Fig. 2) of the basin supports our idea that the tufa genesis is connected down to lineamentic faults in the basement. More precisely, tufa deposits are preferentially located along fracture traces, either immediately above extensional fissures or in the hanging wall of normal faults (Hancock et al., 1999, Piper et al., 2007). Hence, the distribution of the tufa at surface may delineate the fault distribution at depth and/or shows areas with increased basement fracturation.

Based on this hypothesis, a combined geophysical survey has been conducted to answer the following questions:

i) The tufa morphology (cones, pinnacles or bedded elongated structures along fissure ridges)
ii) The present day hydrothermal regime/activity
iii) Depth ranges of the tufa deposits

TUFA & TRAVERTINE

Referring to Hanckock et al. (1999), tufa and travertine are both 'freshwater' limestone deposits originated from springs or other waters that are supersaturated with calcium carbonate. There are gradations among the two rock types. Based on their texture they can be identified: tufa is a name that is usually used to describe a porous and bedded deposit originated from either cold springs or accumulating in veins or lakes. Travertine is a limestone of compact and white texture generated by hydrothermal hot-springs (Hancock et. al, 1999). Due to Hanckock's (1999) analysis of deposits in the Mygdonian Basin in the same area, we name this outcropping rock type tufa. Tufa cones as shown in Fig. 2 form in and on unconsolidated sediments of past and present lake floors where the sediments overly fissure (Fig. 3) in bedrocks (Hancock et. al, 1999). In regions of neotectonism, tufa/travertine preserves a layered signature reflecting the past earthquake activity (Piper et al., 2007)

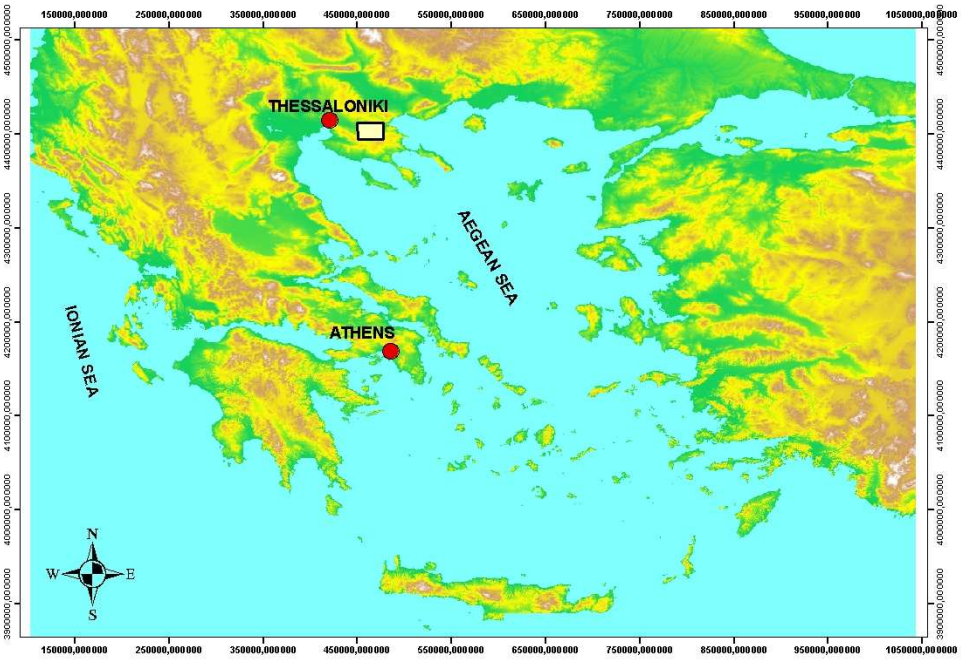

Figure 1: Map of the Aegean See with the location of the survey area (white box).

Figure 2: Tufa cones in the northern part of the Mygdonian Basin. View to the northeast with the village Profitis in the background.

GEOPHYSICAL SURVEY

Limestone deposits such as tufa and travertine exhibit low magnetization (Piper et. al, 2007) but can show high resistivities compared to their host sediments. Especially the lacustrian tufa is generally so porous that if it is above the water table it is almost dry and is hence very high resistive (Ian Hill, pers. comm., 2007).
The analysis of VES soundings (EUROSEISTEST, 1995) along the profile Stivos-Profitis already stated shallow high resistive thin and inhomogeneous layers that have been associated with travertine (tufa) and causes noise in the data acquisition. Hence, near surface resistivity methods are promising tools to detect these rock types.

During 2007, near surface EM geophysical soundings (Tab. 1) have been conducted to study tufa outcrops in Mygdonian Basin. Figure 4 shows the RMT/CSTAMT site location along two Profiles (1&2). Profile 1 is part of the Profile Stivos-Profitis, as referred in the EUROSEISTEST (1995) report for this area. In order to investigate near surface structures with high resolution and the present day geothermal regime, additional VLF (Müller, 1982b; Stiefelhagen, 1998) and self-potential (SP) data were obtained along a road that defines Profile 1.

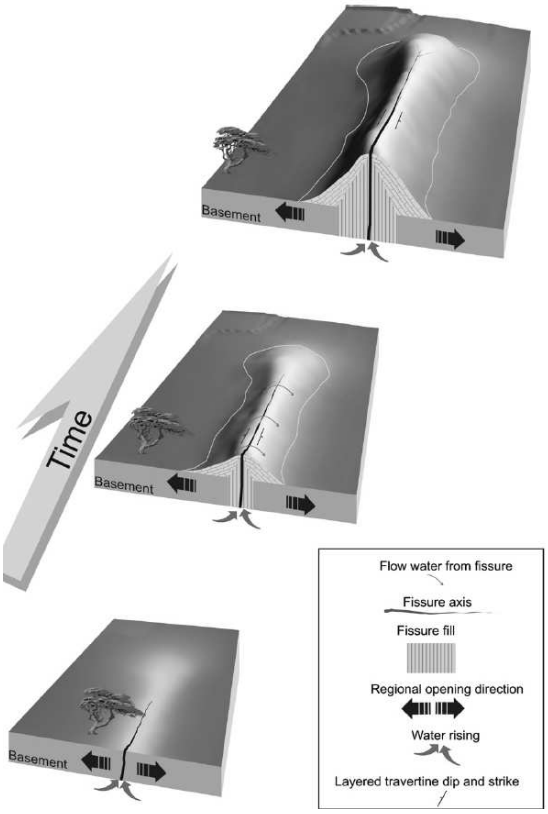

Figure 3: Successive stage of the formation of a travertine mound above an extensional fissure (Piper et. al., 2007; Mesci, 2004)

Method	Sampling	Device	Freq. range
SP	dx =10 m	Ag/AgCl electrodes Gurk (2007)	
RMT/ CSTAMT	dx=50 m or more	ENVIROMT Bastani (2001)	1-250 kHz
VLF	10 Hz	CHYN Müller (1982a)	19.6 kHz

Table 1: List of sounding parameter.

RMT/CSTAMT soundings:
The soundings were carried out along both profiles. A remotely controlled double horizontal magnetic dipole transmitter that is located at certain distances provides the signals for the CSTAMT data. Time series in the RMT and CSTAMT band are processed in the field up to sounding curves allowing to reject data and to repeat the measurement if necessary. Generally data are collected every 50 m along the profile 1. On profile 2, this distance is extended or shortened, if necessary.

Continuously VLF sounding:
Prior to the soundings, we set up marks every 50 m along the profile to assure a good reference to the RMT/CSTAMT measurements. A 19.6 kHz transmitter located at an azimuth of 270°N was chosen to collect VLF data along profile 1. Depending on the walking speed, the sampling rate of 10 Hz will allow for a lateral resolution of about 50 cm. The skin depth is of about 23 m assuming a half space of 40 Ω m.

SP data:
For this study we used Ag/AgCl electrodes arranged on a spade stick. One electrode is kept fixed, whereas the other electrode sampled the potential field on profile 1 every 10 m.

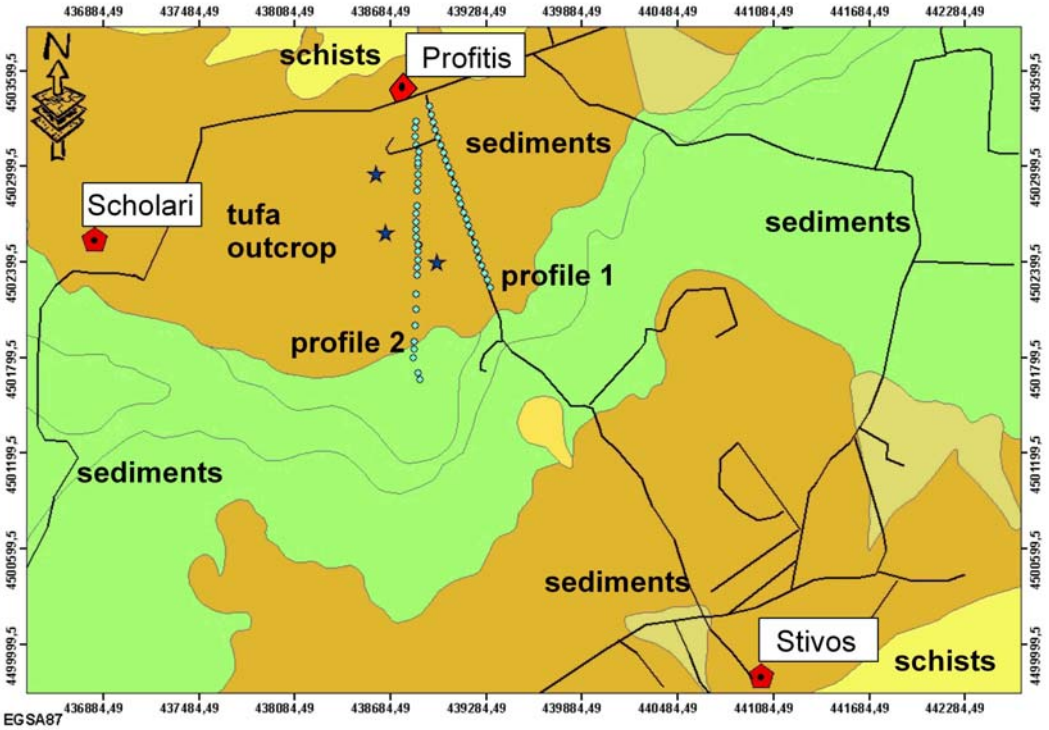

Figure 4: Map of the study area with tufa outcrops (stars) and RMT&CSTAMT site locations (dots). Black lines indicate major roads.

DATA PROCESSING & ANALYSIS

RMT/CSTAMT data are preprocessed in the field. Normally, no further processing steps are reqcuired. The data are available as EDI MT SECT files (Wight, 1987) including GDS data.
To invert the data within the 2D approach we followed the strategy suggested in (Pedersen & Engels, 2005). At this stage, we confine ourselves to analyse Berdichevsky Invariant data (Berdichevsky et al., 1976) which has advantages compared to bi-modal data in 2D inversion. Any variability in strike direction with period does not affect the results as much as for bi-modal inversion, when the proper mode decomposition is vital.
The 2D inversion routine by Siriponvaraporn and Egbert (Siriponvaraporn & Egbert, 2000) has been used to invert the Berdichevsky Invariant data without any topographic correction. As the error floor, we used the standard deviation of the impedance tensor.

The SP data are drift corrected and the VLF data files are corrected with respect to their location along the profile. Since the quadrature of the VLF soundings are less effected by shaking the antenna while walking, we present these data in the following text.

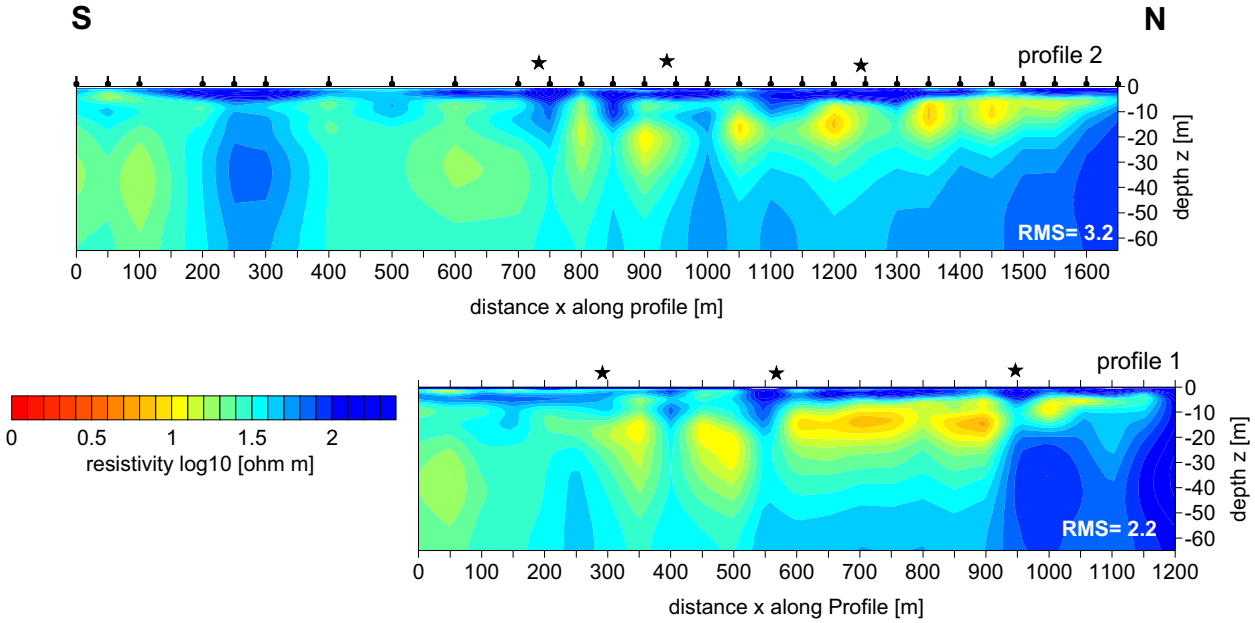

Figure 5: 2D resistivity (Berdichevsky Invariant) cross sections of profile 1&2. Stars indicate projected location of tufa outcrops onto the profiles.

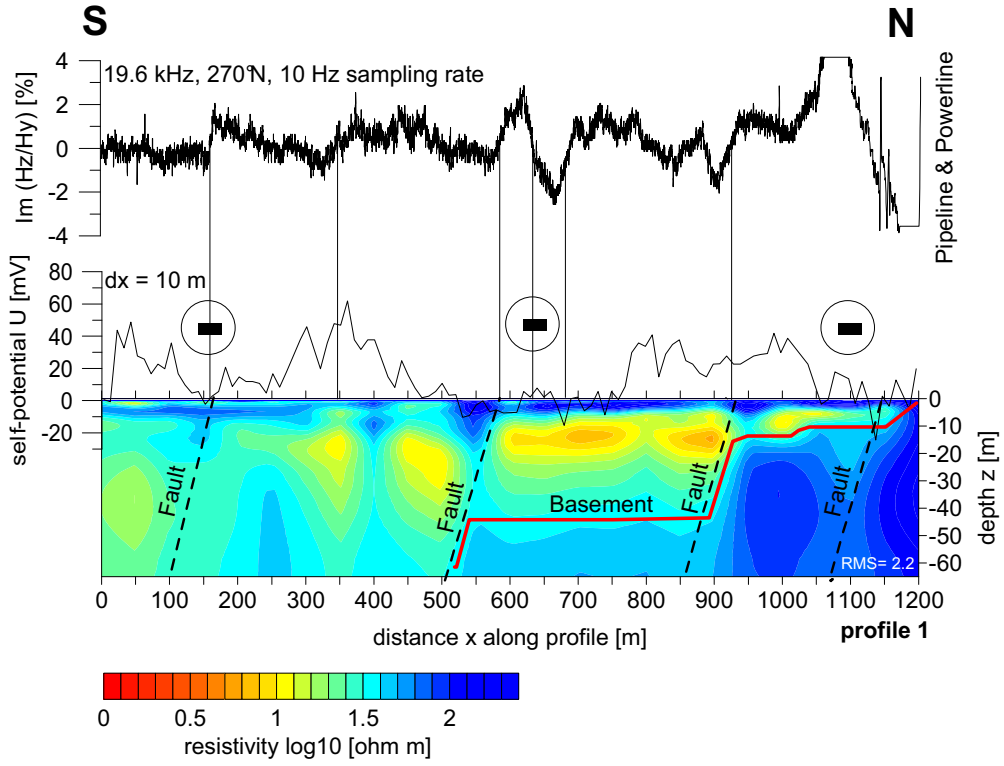

Figure 6: 2D resistivity (Berdichevsky Invariant) cross section of profile 1 together with VLF and SP data. Possible fault locations are presented with dashed lines and assumed basement topography with red lines.

Figure 5 shows results of the 2D inversion for both profiles. Near to the surface (0 to -10 m), we see a series of conductive and high resistive thin layers uneven distributed along the profile. At this stage of investigation, we directly associate the resistive layers with the travertine/tufa rocks and the conductive layers as quaternary sediments. At larger depth, good conductive structures, sometimes interrupted, are predominant followed by the resistive basement rock. Due to the limited skin depth of the EM fields used, the basement is only recognisable at the northern part of the profile where it actually crops out.
Unlike to what we would expect on a consolidated former lacustrian floor, the resistivity structures and therefore the bedding of the sediments are disrupted – and we think, because of the evolving tufa rocks. This idea is supported by the VLF and SP data as sketched out in Fig. 6. Major inflection points in the VLF sounding are superimposed to structural discontinuities in the resistivity cross-section of line 1 indicating strong lateral contrast in conductivity. Those contrasts are likely to be caused by vertical structures such as travertine/tufa pinnacles and faults as sketched out in Fig. 6.
Following the model of Revil & Pezard (1998) in Fig. 7, we are able to identify areas of negative (admittedly, quite weak) self potentials (Fig. 6) on profile 1. They can be addressed to recharge areas at locations where near surface resistive structures are modeled and where major VLF anomalies are present.

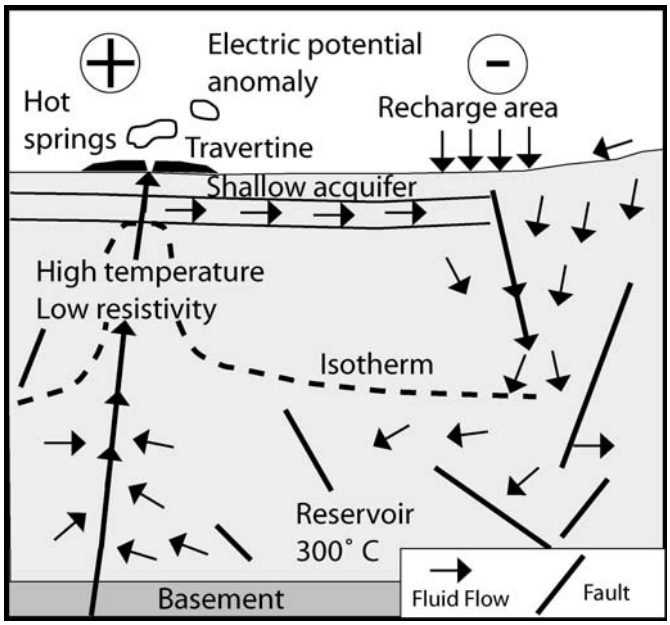

Figure 7: Sketch of a natural thermo-electrokinetik battery (after Revil & Pezard, 1998)

CONCLUSIONS

Supersaturated calcium carbonate hot waters (maybe generated from the marble bands) have followed fissures and fault pathways in the basement and in the unconsolidated lacustrian sediments to create tufa cones and patches of tufa outcrops at surface (Fig. 7). Repeatedly, they became covered by new lacustrian and/or alluvial sediments. Due to a neotectonic seismic event, the geothermal regime changed and the faults that allowed hot water to rise on surface in the past became now preferred pathways for groundwater recharge.
Regarding the morphology of the tufa rocks, we conclude that they cover areas as embedded layers above fissures with possible pinnacle like roots at depth which remain as a more competent rock after erosion processes. The present day depth range of the embedded tufa structures is approx. 0 to -10 m. It is possible that subsequent travertine/tufa layers report revolving changes in the geothermal regime caused by seismic events. Tufa outcrops do indicate areas with increased basement fracturation and may be used to delineate lineamentic structures at depth.
From a hydrogeological point of view, recharge areas as indicated in Fig. 6 are potential drill locations for groundwater production (e.g. at profile location x= 600 m and 900 m).

ACKNOWLEDGEMENTS

This study is supported by the project of the Marie Curie Action ITSAK-GR (International Transfer of Seismological Advanced Knowledge – Geophysical Research), MTCD-CT-2005-029627. We are greatly indebted to the students from Thessaloniki and Crete who took part in the fieldwork. We thank Dr. Pierre-André Schnegg from the University of Neuchâtel for providing us with the VLF device. Finally we would like to thank Lars Dynesius for all his technical help and support during the field measurements.

REFERENCES

Bastani, M., (2001). EnviroMT - A New Controlled Source/Radio Magnetotelluric System. Ph. D. thesis. Acta Universitatis Upsaliensis, Uppsala Dissertations from the Faculty of Science and Technology 32.

Berdichevsky, M.N. and Dmitriev, V.I., (1976), Basic principles of interpretation of magnetotelluric sounding curves, *in Adam A., Ed., Geoelectric and geothermal studies*: Budapest, Akamdemai Kiado, 165-221.

EUROSEISTEST, (1995): 'Volvi-Thessaloniki: A European Test Site for Engineering Seismology, Earthquake Engineering & Seismology', Final Scientific Report, October 1995.

Goldsworthy, M., J. Jackson and J. Haines (2002). The continuity of active fault systems in Greece, Geophys. J. Int., 148, 596–618

Gurk, M. (2007). Eigenpotentialsonde zur schnellen Messung der elektrischen Potentialverteilung und der Langzeitmessung des erdelektrischen Feldes, Gebrauchsmuster Nr. 20 2007 003 079.1. Deutsches Patent und Markenamt, Muenchen.

Hancock, P. L., R. M. L. Chalmes, E. Altunel and Z. Cakir, (1999). Travitonics: using travertines in active fault studies, Journal of Structural Geology, 21, 903-916.

Karagianni, E.E., D.G. Panagiotopoulos, C.B. Papazachos, and P.W. Burton (1999). A study of shallow crustal structure in the Mygdonia Basin (N. Greece) based on the dispersion curves of Rayleigh waves. Journal of the Balkan Geophysical Society, Vol. 2, No 1, 3-14.

Mesci, B.L., (2004). The Development of Travertine occurences in Sıcak, Cermik, Delikkaya and Sarıkaya (Sivas) and their Relationships to Active Tectonics. PhD thesis. Cumhuriyet University, Sivas, Turkey, p. 245 (Unpublished, in Turkish with English abstract).

Müller, I. (1982a). Premières prospections électromagnétiques VLF (very low frequency) dans le karst en Suisse. 7e congrès national de spéléologie, Suisse.

Müller, I. (1982b). Role de la prospection électromagnétique VLF (Very Low Frequency) pour la mise en valeur et la prospection des aquifères calcaires. Annales Scintifiques de l' Université de Besancon 1: 219-226.

Papazachos, B.C., Mountrakis, D., Psilovikos, A., and Leventakis, G., (1979) 'Surface fault traces and fault plane solutions of the May-June 1978 major shocks in the Thessaloniki area, Greece', Tectonophysics, 53, 171-183.

Pedersen, L.B. and Engels, M. (2005). Routine 2D inversion of Magnetotelluric data using the determinant of the impedance tensor. Geophysics 70, G33-G41.

Piper, J.D., Levent B. Mesci, Halil Gürsoy, Orhan Tatar and Ceri J. Davies, (2007). Palaeomagnetic and rock magnetic properties of travertine: Its potential as a recorder of geomagnetic palaeosecular variation, environmental change and earthquake activity in the Sıcak Cermik geothermal field, Turkey, Physics of the Earth and Planetary Interiors 161, 50–73

Raptakis D., Manakou M., Chavez-Garcia F., Makra K., Pitilakis K., (2005). 3D configuration of Mygdonian basin and preliminary estimate of its site response, Soil dynamics and Earthquake Engineering, 25, 871-887.

Revil, A. & P. A. Pezard, (1998). Streaming Electrical Potential Anomlay Along Faults in Geothermal Areas, Geoph. Res. Let., 25, 3197-3200

Savvaidis, A. Pedersen, L. B., Tsokas, G. N., Dawes, G. J., (2000). Structure of the Mygdonian Basin (N. Greece) inferred from MT and gravity data, Tectonophysics, 317, 171-186.

Siripunvaraporn W. and Egbert G, (2000). An efficient data-subspace inversion method for 2-D magnetotelluric data. Geophysics, 65, 791–803.

Stiefelhagen, W. (1998). Radio Frequency Electromagnetics (RF-EM): Kontinuierlich messendes Breitband-VLF, erweitert auf hydrogeologische Problemstellungen. PhD Thesis, Centre of Hydrogeology. Neuchâtel, Switzerland, University of Neuchâtel, pp. 243.

Weight, D. E., (1987), MT/EMAP Data Interchange Standard, Society of Exploration Geophysicists, pp.72.